CXCL13 inhibition induce the apoptosis of MDA-MB-231 breast cancer cells through blocking CXCR5/ERK signaling pathway

J.-J. MA, L. JIANG, D.-Y. TONG, Y.-N. REN, M.-F. SHENG, H.-C. LIU

Department of Oncology, the People's Liberation Army 107 Hospital, Yantai, Shandong, P.R. China

Jianjun Ma and Li Jiang contributed equally to this work

Abstract. – OBJECTIVE: Treatment of the high-risk triple negative breast cancer (TNBC) is a critical clinical challenge. Here we aimed to explore a novel strategy for TNBC treatment by blocking the tumor-associated chemokine CXCL13 in the MDA-MB-231 TNBC cells.

MATERIALS AND METHODS: MDA-MB-231 cells were treated with anti-CXCL13 antibodies (inhibition group), or phosphate-buffered saline (PBS) (control group), followed by determining the levels of interleukin-1 (IL-1), tumor necrosis factor-alpha (TNF-α) and transforming growth factor beta-1 (TGF-β1) with enzyme-linked immunosorbent assay (ELISA). The effects of CXCL13 inhibition on cell proliferation and apoptosis were assessed by 3-(4,5-dimethylthiazol-2-yl)-2,5-diphenyl tetrazolium bromide (MTT) assay and flow cytometry, respectively. Quantitative Real Time-PCR (qRT-PCR) and Western blot were used to compare the levels of CXCL13, CXCR5, extracellular signal-regulated kinase (ERK). The levels of cyclin D1 and cleaved caspase-9 were detected by Western blot.

RESULTS: The levels of IL-1, TNF-α and TGF-β1 in MDA-MB-231 cells treated with anti-CXCL13 antibodies were significantly downregulated (*p*<0.05). Meanwhile, CXCL13 blockade decreased the cell proliferation and increased the apoptosis rate of MDA-MB-231 cells. The inhibition of CXCL13 led to marked reduction in CXCL13 and CXCR5 mRNA and an increase in ERK mRNA. The inhibition of CXCL13 resulted in the downregulation of CXCL13, CXCR5, p-ERK/ERK, cyclin D1 and upregulation of cleaved caspase-9 proteins.

CONCLUSIONS: CXCL13 blockade effectively suppressed the proliferation of MDA-MB-231 cells by promoting cell apoptosis. This effect is presumably associated with the downregulation of CXCL13 and suppression of the CXCR5/ERK signaling pathway.

Key Words:
    CXCL13, Breast cancer, CXCR5/ERK, CXCR.

Introduction

Breast cancer is one of the most common cancers among women worldwide[1]. Despite recent advances in breast cancer screening and treatment, the survival rate of patients with metastatic breast cancers remains dismal[2]. Existing therapies, such as chemotherapy and radiotherapy, have not achieved a satisfactory clinical outcome for late-stage breast cancer patients, prompting the search for new therapeutic targets and strategies to effectively impede worsening of late-stage tumors. One promising class of such targets is found in the tumor microenvironment, such as extracellular matrix molecules, fibroblasts, immune cells, inflammatory factors, etc., which form an environment favorable to the proliferation, migration and invasion of cancer cells[3]. Chemokines were originally considered to govern the movement of lymphocytes in immune responses. New evidence indicated that chemokines are important regulators of the proliferation, migration and metastasis of cancer cells, promoting cancer progression[4]. The overexpression of chemokines in an autocrine pathway has been found in a large array of cancers, including prostate cancer[5], colorectal cancer[6] and breast cancer[7]. Trafficking of B- and T- cells to tumor microenvironment has also been linked to autocrine pathways, which has a significant role in cancer cell migration. The chemokine/receptor interaction also plays a critical part in the activation of many oncogenic intracellular signaling pathways[8,9]. There were more than 40 chemokines in human, of which the 'CXC' chemokines are defined by the presence of a single amino acid residue flanked by two cysteines[7]. The CXCL13-CXCR5 axis is a putative molecular pathway in cancer progression.

Corresponding Authors: Mengfei Sheng, MD; e-mail: shengmengfei04@163.com
Hanchen Liu; e-mail: 49463515@qq.com

CXCR5 is the receptor of chemokine CXCL13; the expression of CXCL13 and CXCR5 are both greatly elevated in cancers[5,6]. Of note, their upregulation was found to be highly correlated with advanced disease and potentially predictive of the poor survival of patients[5,6,10]. Findings on this chemokine-driven tumor progression gave rise to recent endeavors in utilizing anti-chemokine strategies to throttle the progression of cancers. For example, anti-CXCL13 neutralizing antibodies were used to counteract the migration of breast cancer and neuroblastoma cells[8,11]. However, this CXCL13 inhibition strategy has not been systemically studied in breast cancer and there is no clear evidence of its effectiveness in breast cancer treatment. Herein, the purpose of this study is to characterize the efficiency of the CXCL13 inhibition in regulating the proliferation and apoptosis of a triple-negative breast cancer cell line, MDA-MB-231. We focused on the CXCR5/ERK pathway to elucidate the mechanism of this anti-tumor strategy.

Materials and Methods

Cell Culture

The human triple-negative breast cancer cell line MDA-MB-231 was purchased from the American Type Culture Collection (ATCC; Manassas, VA, USA). Cells were cultured in Dulbecco's Modified Eagle Medium (DMEM; Gibco, Grand Island, NY, USA) containing 100 μg/mL Streptomycin, 100 IU/mL penicillin and 10% fetal bovine serum (FBS) in 37 °C and 5% CO_2. Cells were collected at logarithm phase for further experiments. CXCL13 inhibition was performed by adding 30 μL CXCL13 antibody (20 μg/mL, dissolved in PBS, cat# 300-47, PeproTech., Rocky Hill, NJ, USA); the concentration of CXCL13 antibody was 60 ng/mL. Cell in the control group was added the same volume PBS.

Cell Viability Assay

MTT assay was used to assess cell viability. MDA-MB-231 cells (2×10^3 per well) were seeded into 96-well plates. Cells were allowed to attach the plate for 12 h and incubated for another 24 h after CXCL13 antibodies were added. Following this, 10 μL of MTT reagent (5 mg/mL) was added and incubated for another 4 h in 37°C, 5% CO_2. After removing culture medium, 150 μL of dimethyl sulfoxide (DMSO) was added; the plate was shaken in the dark for 15 min. Then, the optical density (OD) values were measured at the absorbance of 490 nm by a SpectraMax 190 Microplate Reader (Molecular Devices, San Jose, CA, USA). The cell viability was calculated using the following equation: cell viability = $(OD_{treated}-OD_{blank})/OD_{control}-OD_{blank})\times100\%$.

Cell Apoptosis

Cell apoptosis was analyzed by flow cytometry. Cells were trypsinized, collected and counted. 1×10^6 cells were washed with cold 1×PBS twice and centrifuged at 1000 rpm for 5 min. Then, cells were re-suspended in 100 μL of 1×binding buffer, followed by adding 5 μL Annexin V-fluorescein isothiocyanate (FITC) and 5 μL propidium iodide (PI). After incubation for 15 min, 400 μL 1×binding buffer was added and the cell suspension was measured by flow cytometry (CyFlow Cube, CyFlow Ploidy Analyser, Munster, Germany).

Enzyme-Linked Immunosorbent Assay

ELISA was used to analyze the levels of IL-1, TNF-α and TGF-β1. At 18 h after CXCL13 were added, the cells were centrifuged at 1000 rpm for 10 min and the supernatant was collected. ELISA was performed in accordance to manufacturer's instruction of the kits for IL-1 (AB46052, Abcam, Cambridge, MA, USA), TNF-α (ABIN491828, Cloud-Clone Corp., Houston, TX, USA) and TGF-β1 (AB100647, Abcam, Cambridge, MA, USA).

Quantitative Real Time-PCR Analysis

The TRIzol kit (Invitrogen, Carlsbad, CA, USA) was used to extract total RNA from cells. RNAs were then reverse-transcribed to cDNA using the SuperScript III Reverse Transcriptase (Thermo Fisher Scientific, Waltham, MA, USA). PCR was performed using Master ep realplex2 (Eppendorf, Hamburg, Germany) using the following conditions: 95°C for 30 s, 95°C for 5 s, and 60°C for 45 s (40 cycles). The $2^{-\Delta\Delta Ct}$ method was used for data analysis. β-actin mRNA was used as the internal control. Primer sequences used are listed in Table I.

Western Blot

Cell lysate was centrifuged at 2000 rpm for 20 min to collect the supernatant. BCA kit (Beijing Solarbio Science & Technology Co., Ltd, Beijing, China) was used to quantify protein concentration. 4 μl of protein lysate was diluted using the 5× sample buffer and loaded to 10% gel of sodium dodecyl sulphate-polyacrylamide gel electrophoresis (SDS-PAGE) at 80 V. Proteins were then
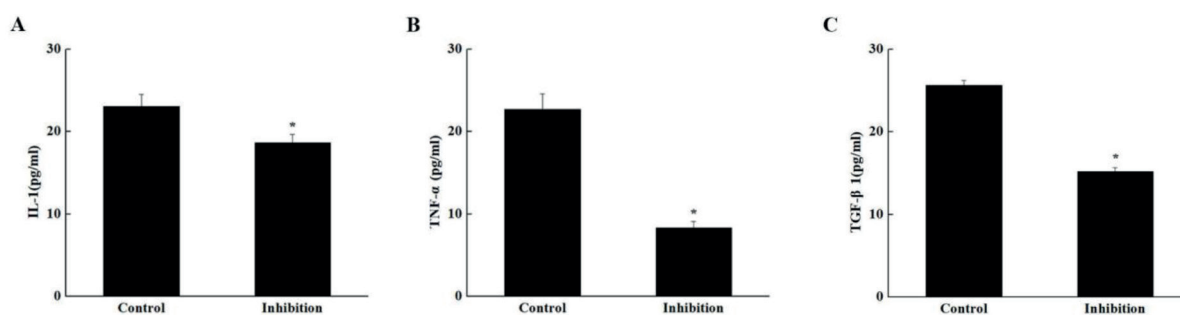
Figure 1. CXCL13 inhibition attenuated expression of inflammatory factors and TGF-β1. The levels of IL-1 *A,* TNF-α *B,* and TGF-β1 *C,* in control and inhibition groups were measured by ELISA analysis. *$p<0.05$ *vs.* control group.

transferred to polyvinylidene difluoride (PVDF) membranes (Merck, Darmstadt, Germany), followed by using 5% skim milk powder to block the membrane for 2 h. The rabbit anti-CXCL13 antibody (1:1000, ABIN3030506, NSJ Bioreagents, San Diego, CA, USA), CXCR5 (1:1000, ABIN1881245, Abgent, San Diego, CA, USA), ERK (1:1000,M00104-1, Boster, Pleasanton, CA, USA), β-actin (1:1000,ab8226, Abcam, Cambridge, MA, USA), p-ERK (1:1000, PA2026, BosterBio, Pleasanton, CA, USA), cyclin D1 (1:1000, ABIN2779291, Aviva Systems Biology, San Diego, CA, USA), and Cleaved caspase-9 (1:1000, #20750, Cell Signaling Technology, Danvers, MA, USA) were then added and incubated at 4°C overnight. The goat anti-rabbit IgG-HRP (1:1000, MBS435036, MyBioSource, San Diego, CA, USA) was then added and incubated at room temperature for 1h. The Elecsys-2010 (Roche, Basel, Switzerland) was used to acquire the blot image. β-actin was used as a loading control. Image J software (NIH) was used to quantify the protein expression.

Statistical Analysis

SPSS19.0 was used for statistical analysis. Data were presented as mean±SD. The comparison between the two groups was conducted using Student's *t*-test. The comparison between more than two groups was performed using one-way analysis of variance (ANOVA). The LSD method was applied in the comparison between the two groups. Differences with $p<0.05$ were considered statistically significant.

Results

CXCL13 Inhibition Downregulated Expression of Inflammatory Factors and TGF-β1

Since CXCL13 is a putative inflammatory regulator, we first evaluated how CXCL13 blockade affected the expression of inflammatory factors and TGF-β1 in MDA-MB-231 cells. As shown in Figure 1, IL-1, TNF-α and TGF-β1 expression was lowered by approximately 19.1%, 63.3% and 40.7% in MDA-MB-231 cells treated with CXCL13 inhibitor compared to those in untreated cells ($p<0.05$). This is consistent with the tumor-promoting role of CXCL13 as inflammatory factors and TGF-β1 are potent oncogenic factors secreted by cancer cells. Therefore, we hypothesized that the inhibition of CXCL13 is likely a viable strategy to suppress bre-

Table I. Primer sequences.

Name	Sequence
CXCL13	Forward:5′-GCTTGAGGTGTAGATGTGTCC-3′
	Reverse: 5′-CCCACGGGGCAAGATTTGAA-3′
CXCR5	Forward:5′-GGTCACCCTACCACATCGTC-3′
	Reverse: 5′-GCCATTCAGCTTGCAGGTATTG-3′
ERK	Forward:5′-CGGGGCATCTTCGAGATCG-3′
	Reverse: 5′-CAGAACAACGCCGTTTCAGTT-3′
β-actin	Forward:5′-TAGGCCGTGGCTCAAGAAC-3′
	Reverse: 5′-TGCATCTCCAAGTTGCCTTTG-3′
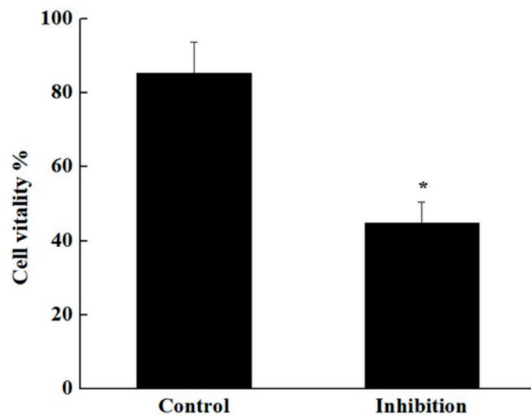
Figure 2. CXCL13 inhibition attenuated MDA-MB-231 cells viability. The cell viability of MDA-MB-231 cells with or without CXCL13 antibodies was analyzed by MTT assay. *$p<0.05$ *vs.* control group.

ast cancer progression.

CXCL13 Inhibition Decreased the Viability and Promoted the Apoptosis of MDA-MB-231 Cells

To verify the effects of the CXCL13 inhibition on suppressing breast cancer progression, we first tested whether the CXCL13 inhibition was able to decrease the viability of MDA-MB-231 cells. As shown in Figure 2, the CXCL13 inhibition caused a marked reduction of cell viability (40.61%) ($p<0.05$). Based on this, we then proceeded to test whether CXCL13 promoted cell apoptosis. Flow cytometry analysis of cells after Annexin-V-FITC/PI staining (Figure 3A) suggested a dramatically increased apoptosis rate with CXCL13 inhibition (Figure 3B). This evidence clearly indicated that the CXCL13 inhibition exerted anti-tu-

mor effects in MDA-MB-231 cells.

CXCL13 Inhibition Suppresses Survival Protein Expression and Increase Cell Apoptosis Protein Expression

To elucidate the suppressive effects of CXCL13 inhibition on the cell survival, we next examined how CXCL13, CXCR5, p-ERK/ERK, cyclinD1 and cleaved caspase-9 expression changed after CXCL13 inhibition. As shown in Figure 4, it was verified that the CXCL13 inhibition resulted in a marked decrease in CXCL13 protein levels (Figure 4A and 4B). Concomitantly, CXCR5, p-ERK/ERK and cyclin D1 demonstrated a significant decrease after the CXCL13 inhibition, while cleaved caspase-9 exhibited a significant upregulation (Figure 4A, C-F). The decreased mRNA levels of CXCL13 (Figure 5A), CXCR5 (Figure 5B) and increased mRNA level of ERK (Figure 5C) further verified this observation. Collectively, these data indicated that the oncogenic CXCR5/ERK signaling pathway was attenuated by CXCL13 inhibition. The decrease of the survival protein, cyclin D1 and the increase of apoptosis protein cleaved caspase-9 were consistent with the proliferation inhibition and apoptosis upregulation.

Discussion

In the present study, we confirmed that CXCL13 blockade is an effective strategy in suppressing breast cancer proliferation and inducing cell apoptosis. We confirmed that the pro-inflammatory factors IL-1, TNF-α and a key growth factor TGF-β1 were concomitantly downregulated by the CXCL13 inhibition. Our motivation for
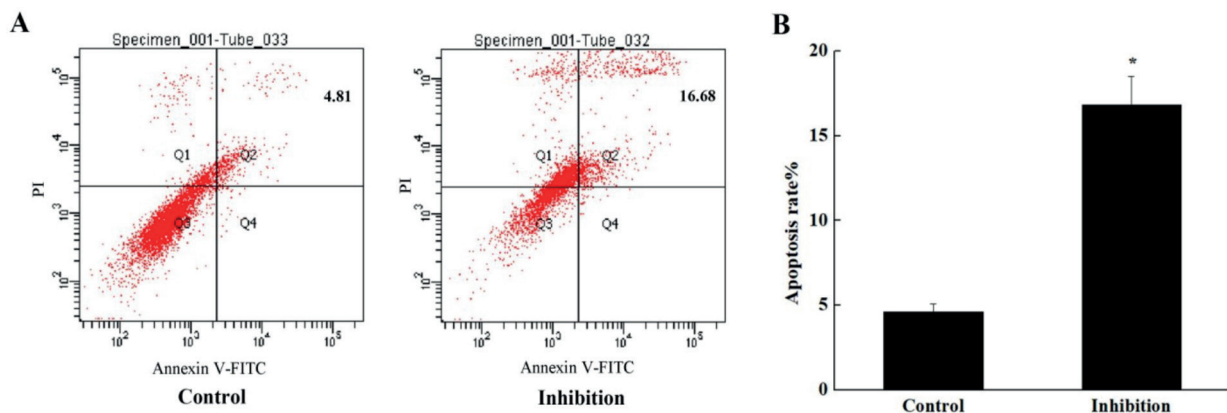
Figure 3. CXCL13 inhibition promotes cell apoptosis. *A,* Representative flow cytometry graphs of MDA-MB-231 cells with or without CXCL13 inhibition, analyzed after Annexin V-FITC/PI staining. *B,* Quantitative comparison of apoptosis in untreated or CXCL13-inhibitor-treated MDA-MB-231. *$p<0.05$ *vs.* control group.
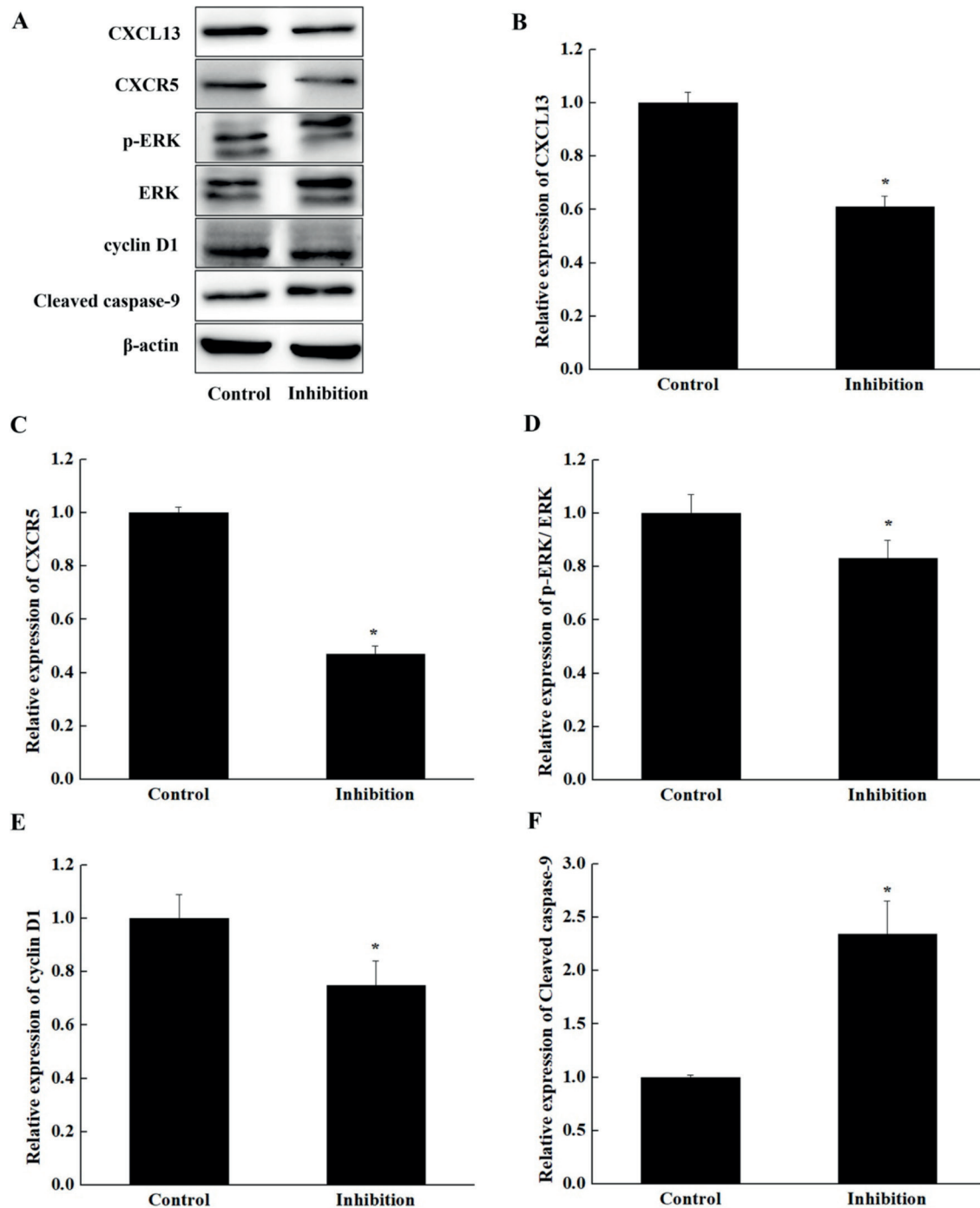
Figure 4. CXCL13 inhibition suppressed the expression of survival protein and increased proteins related to cell apoptosis. *A,* Representative Western blot showed the decrease of CXCL13, CXCR5 and cyclin D1, and the increase of p-ERK, ERK and cleaved caspase-9 after CXCL13 inhibition. Quantitative comparison of CXCL13 *B,* CXCR5 *C,* p-ERK/ERK *D,* cyclin D1 *E,* and cleaved caspase-9 *F,* in MDA-MB-231 cells with or without CXCL13 inhibition. *$p<0.05$ *vs.* control group.

investigating inflammatory factors stems from the two viewpoints that inflammatory cytokines are regulated by chemokines[12] and chemokine reduction also diminishes inflammation[13]. This in-triguing approach has ameliorated heart functions by blocking CCL5 and CXCL4 and inducing in-flammation reduction[13]. Notably, the CXCL13 neutralization approach has been widely employed
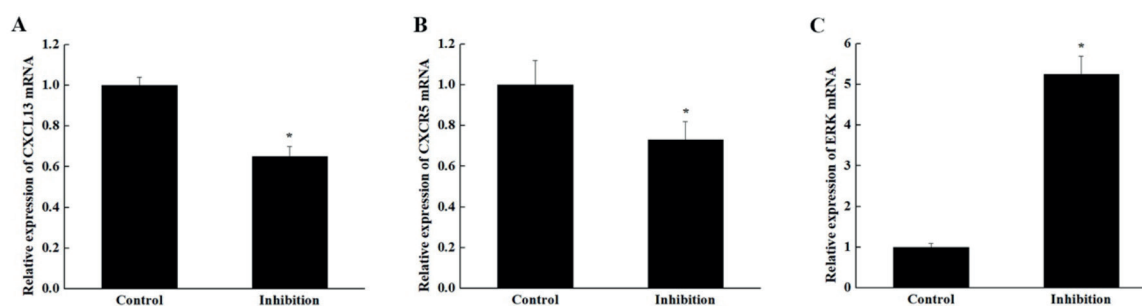
Figure 5. CXCL13 inhibited CXCL13, CXCR5 and increased ERK expression in mRNA levels measured by qRT-PCR analysis. qRT-PCR analysis of CXCL13 *A*, CXCR5 *B,* and ERK *C,* mRNA expression in inhibition and control group. *$p<0.05$ *vs.* control group.

for the management of autoimmune diseases, as Zheng et al[14] reported that CXCL13 neutralization reduces the severity of collagen-induced arthritis. Consistent with our result, the CXCL13 inhibition was shown to result in attenuated inflammatory cytokine production. In addition, our data corroborated the key role of CXCL13 in secondary lymphoid tissue orchestration and lymphoid neogenesis[15] by mediating the germinal center response and trafficking of B- and T-cells[16,17]. TGF-β1 functions both as a tumor suppressor and as a promoter. Under normal condition, TGF-β1 regulates tissue homeostasis by coordinating apoptosis and inhibiting incipient tumor growth. However, during tumor progression, TGF-β1 served as a promoter of epithelial-to-mesenchymal transition (EMT) and was resistant to cell death[18]. Tumor cells also secrete TGF-β1 as a way to induce EMT and hijack the immune system for dissemination. The CXCL13 expression is also associated with EMT in breast cancer and considered accountable for the metastases formation[19]. The triple-negative MDA-MB-231 cells are known as post-EMT cells with high metastatic potential[20]. The suppression of TGF-β1 is consistent with the antitumor function of the CXCL13 inhibition. We next showed that the proliferation of MDA-MB-231 cells was suppressed by the CXCL13 inhibition, while the apoptosis was promoted. This finding was further supported by the decrease of cyclin D1, a cell cycle regulator, and cleaved caspase-9, an apoptosis marker. Currently, there were very few reports about the use of the CXCL13 inhibition strategy for the treatment of autoimmune diseases, colorectal and prostate cancers[4-6,21]. In breast cancer, only a few studies have proposed the correlation between the CXCL13 expression and breast cancer EMT and poor diagnosis of patients[7,19,22]. Our study provides a valuable tool to impede the progression of this

highly aggressive disease by CXCL13 inhibition. However, our data are limited to *in vitro* inhibition effects. Further investigation about the role of the CXCL13 inhibition to suppress breast cancer progression *in vivo* will be highly valuable. We showed that the CXCR5 expression was also reduced upon CXCL13 inhibition. This result is in line with the role of CXCR5 transduction in the regulation of intracellular oncogenic pathways[10]. p-ERK/ERK was significantly decreased in cells with CXCL13 inhibition, suggesting attenuated ERK signaling. Echoing this, El-Haibi et al[23] demonstrated that CXCL13 mediates prostate cancer cell proliferation through the JNK signaling and invasion through the ERK activation. ERK signaling has been shown to regulate breast cancers by transcription induction of Zeb1 and nuclear accumulation of unphosphorylated (active) β-catenin[24], thereby driving the expansion and tumorigenesis of cancer cells. Our findings implicated that CXCL13-CXCR5 axis is an upstream regulator of ERK signaling. It should be noted that the anti-tumor effect of the CXCL13 inhibition may not be merely originated from its regulation of ERK signaling. As previous studies indicated, PI3K/AKT and PTEN pathways may also be other mechanisms of the CXCL13 regulation[10,25]. For *in vivo* treatment, the physiological responses to the CXCL13 inhibition may be more complex. For example, the regulation of chemokines is highly correlated with cancer immunotherapy, whereby the participation of a large variety of immune cells should be meticulously considered[3].

Conclusions

In this work, we proposed the novel anti-tumor strategy of the CXCL13 inhibition for triple-ne-

gative breast cancer MDA-MB-231 cells. We showed that the CXCL13 inhibition led to significant reduction of IL-1, TNF-α and TGF-β1 decreased cell proliferation and increased apoptosis rate. The anti-tumor effect is attributed to the suppression of ERK signaling in breast cancer cells. The data in this work justified that the CXCL13 inhibition could be a potential approach for impeding breast cancer progression.

Conflict of Interest

The Authors declare that they have no conflict of interest.

References

1) Siegel RL, Miller KD, Jemal A. Cancer statistics, 2018. CA Cancer J Clin 2018; 68: 7-30.

2) Hu XL, Wang J, He W, Zhao P, Wu WQ. Down-regulation of lncRNA Linc00152 suppressed cell viability, invasion, migration, and epithelial to mesenchymal transition, and reversed chemo-resistance in breast cancer cells. Eur Rev Med Pharmacol Sci 2018; 22: 3074-3084.

3) Nagarsheth N, Wicha MS, Zou W. Chemokines in the cancer microenvironment and their relevance in cancer immunotherapy. Nat Rev Immunol 2017; 17: 559-572.

4) Singh R, Lillard JW Jr., Singh S. Chemokines: key players in cancer progression and metastasis. Front Biosci 2011; 3: 1569-1582.

5) Han FL, Liang F, Jiang TC, Liu M. Increased expression of CXCR5 and CXCL13 in mice with experimental autoimmune myocarditis. Eur Rev Med Pharmacol Sci 2017; 21: 1860-1867.

6) Qi XW, Xia SH, Yin Y, Jin LF, Pu Y, Hua D, Wu HR. Expression features of CXCR5 and its ligand, CXCL13 associated with poor prognosis of advanced colorectal cancer. Eur Rev Med Pharmacol Sci 2014; 18: 1916-1924.

7) Razmkhah M, Jaberipour M, Safaei A, Talei AR, Erfani N, Ghaderi A. Chemokine and chemokine receptors: a comparative study between metastatic and nonmetastatic lymph nodes in breast cancer patients. Eur Cytokine Netw 2012; 23: 72-77.

8) Pimenta EM, De S, Weiss R, Feng D, Hall K, Kilic S, Bhanot G, Ganesan S, Ran S, Barnes BJ. IRF5 is a novel regulator of CXCL13 expression in breast cancer that regulates CXCR5(+) B- and T-cell trafficking to tumor-conditioned media. Immunol Cell Biol 2015; 93: 486-499.

9) Falkenhagen KM, Braziel RM, Fraunfelder FW, Smith JR. B-Cells in ocular adnexal lymphoproliferative lesions express B-cell attracting chemokine 1 (CXCL13). Am J Ophthalmol 2005; 140: 335-337.

10) Zhu Z, Zhang X, Guo H, Fu L, Pan G, Sun Y. CXCL13-CXCR5 axis promotes the growth and invasion of colon cancer cells via PI3K/AKT pathway. Mol Cell Biochem 2015; 400: 287-295.

11) Airoldi I, Cocco C, Morandi F, Prigione I, Pistoia V. CXCR5 may be involved in the attraction of human metastatic neuroblastoma cells to the bone marrow. Cancer Immunol Immunother 2008; 57: 541-548.

12) Shi Y, Pan H, Zhang HZ, Zhao XY, Jin J, Wang HY. Lipoxin A4 mitigates experimental autoimmune myocarditis by regulating inflammatory response, NF-κB and PI3K/Akt signaling pathway in mice. Eur Rev Med Pharmacol Sci 2017; 21: 1850-1859.

13) Vajen T, Koenen RR, Werner I, Staudt M, Projahn D, Curaj A, Sönmez TT, Simsekyilmaz S, Schumacher D, Möllmann J, Hackeng TM, Hundelshausen PV, Weber C, Liehn EA. Blocking CCL5-CXCL4 heteromerization preserves heart function after myocardial infarction by attenuating leukocyte recruitment and NETosis. Sci Rep 2018; 8: 10647.

14) Zheng B, Ozen Z, Zhang X, De Silva S, Marinova E, Guo L, Wansley D, Huston DP, West MR, Han S. CXCL13 neutralization reduces the severity of collagen-induced arthritis. Arthritis Rheum 2005; 52: 620-626.

15) Finch DK, Ettinger R, Karnell JL, Herbst R, Sleeman MA. Effects of CXCL13 inhibition on lymphoid follicles in models of autoimmune disease. Eur J Clinical Invest 2013; 43: 501-509.

16) Zhao G, Mi JY, Pan XY, Zhang X, Rui YJ. Correlations between CXCL13, IL-24 genes and wrist arthritis. Eur Rev Med Pharmacol Sci 2018; 22: 25-30.

17) Mueller SN, Hosiawa-Meagher KA, Konieczny BT, Sullivan BM, Bachmann MF, Locksley RM, Ahmed R, Matloubian M. Regulation of homeostatic chemokine expression and cell trafficking during immune responses. Science 2007; 317: 670-674.

18) Bu JQ, Chen F. TGF-β1 promotes cells invasion and migration by inducing epithelial mesenchymal transformation in oral squamous cell carcinoma. Eur Rev Med Pharmacol Sci 2017; 21: 2137-2144.

19) Biswas S, Sengupta S, Roy Chowdhury S, Jana S, Mandal G, Mandal PK, Saha N, Malhotra V, Gupta A, Kuprash DV, Bhattacharyya A. Erratum to: CXCL13-CXCR5 co-expression regulates epithelial to mesenchymal transition of breast cancer cells during lymph node metastasis. Breast Cancer Res Treat 2016; 155: 615-616.

20) Carpenter RL, Paw I, Dewhirst MW, Lo H-W. Akt phosphorylates and activates HSF-1 independent of heat shock, leading to Slug overexpression and epithelial–mesenchymal transition (EMT) of HER2-overexpressing breast cancer cells. Oncogene 2015; 34: 546.

21) Ammirante M, Luo JL, Grivennikov S, Nedospasov S, Karin M. B-cell-derived lymphotoxin promotes ca-

stration-resistant prostate cancer. Nature 2010; 464: 302-305.

22) Razis E, Kalogeras KT, Kotoula V, Eleftheraki AG, Nikitas N, Kronenwett R, Timotheadou E, Christodoulou C, Pectasides D, Gogas H, Wirtz RM, Makatsoris T, Bafaloukos D, Aravantinos G, Televantou D, Pavlidis N, Fountzilas G. Improved outcome of high-risk early HER2 positive breast cancer with high CXCL13-CXCR5 messenger RNA expression. Clin Breast Cancer 2012; 12: 183-193.

23) El-Haibi CP, Singh R, Sharma PK, Singh S, Lillard JW. CXCL13 mediates prostate cancer cell prolifera-

tion through JNK signalling and invasion through ERK activation. Cell Prolif 2011; 44: 311-319.

24) Chang CJ, Yang JY, Xia W, Chen CT, Xie X, Chao CH, Woodward WA, Hsu JM, Hortobagyi GN, Hung MC. EZH2 promotes expansion of breast tumor initiating cells through activation of RAF1-beta-catenin signaling. Cancer Cell 2011; 19: 86-100.

25) Garg R, Blando JM, Perez CJ, Abba MC, Benavides F, Kazanietz MG. Protein kinase C epsilon cooperates with PTEN loss for prostate tumorigenesis through the CXCL13-CXCR5 pathway. Cell Rep 2017; 19: 375-388.